Analytical approach to thermodynamics of bolalipid membranes

Sergei I. Mukhin* and Boris B. Kheyfets

Department of Theoretical Physics and Quantum Technologies, Moscow Institute for Steel & Alloys, Moscow, Russia

(Received 5 April 2010; revised manuscript received 2 September 2010; published 1 November 2010)

In this work we derive analytically various thermodynamic properties of bolalipid membranes using microscopic model (elastic strings) and path-integral technique. Among calculated characteristics are lateral pressure profile (with and without hairpin bolalipids), chain orientational order parameter, pressure-area isotherms, coefficient of thermal area expansion, compressibility modulus, and area per bolalipid chain as a function of temperature. Results are compared with our previous ones for a monopolar lipid bilayer and with results of other relevant studies. The limiting case of absolutely rigid strings is also considered. Evaluation of quantum effects is made and found to be negligible.

I. INTRODUCTION

According to Woese *et al.* [1] there are three natural domains of cellular organisms: bacteria, eucarya, and archaea. Some archaea live in extreme conditions: such as high pressure or high temperature, or very high or very low acidity. Archaea membrane has a unique component—so-called bolalipids, which are believed to be responsible for the vitality of archaea. The study of distinctive thermodynamic properties of bolalipid membrane is important since bolaform lipid materials are considered as prospective materials for various research and technological applications [2,3].

Regularly, lipids such as phospholipids or glycolipids are monopolar: having one polar (hydrophylic) "head" and two nonpolar (hydrophobic) "tails" (or "chains"). In contrast to them bolalipids are bipolar [4]: having two polar heads placed on opposing hydrophylic ends of the bolalipid [see Figs. 1(a) and 1(b)]. Monopolar lipids of bacteria and eucarya cell membrane form a bilayer, whereas bipolar lipids of archaea cell membrane form a monolayer with two hydrophylic surfaces. Bolalipids could also have both of their heads at one membrane's interface. In this case they are called hairpin (or U-shaped) bolalipids [see Fig. 1(c)].

Heuristically, bipolar lipid could be thought of as two monopolar lipids with linked tails; compare Figs. 1(a) and 1(b). Within the present model we found (see Sec. II E) that just linking of the tails alone leads to distinctive lateral pressure profile and chain orientational order inside a bolalipid membrane as compared with a monopolar lipid bilayer. Besides, results of our calculations suggest that linking of the tails depletes chain contribution to the coefficient of thermal area expansion and enhances the chain isothermal compressibility modulus (see Table I in Sec. III).

We base on the microscopic model of flexible strings developed in [5], but now we "glue" together the opposite free tails in the membrane midplane in a pairwise fashion. Also, in the present paper we somewhat improved the model and added kinetic-energy term into a chain energy functional studied earlier in [5].

The paper is organized as follows. After an introduction, we describe in Sec. II the application of the flexible strings model to bolalipids and derive the main results including bolalipid orientational order parameter and lateral pressure profiles. We also compare our results for bolalipid membrane with the results obtained earlier for the monopolar lipid bilayer [5]. In Sec. III we compare our results for bolalipid membrane with results for bolalipids and monopolar lipids obtained experimentally [18] as well as obtained with numerical simulation techniques [4,17]. After that, we discuss the case of asymmetrical bolalipid membrane that possesses a finite concentration of hairpin bolalipids. Finally, the limiting case of absolutely rigid strings is considered in order to study behavior of the free energy of a chain under an increase in its (effective) rigidity. In appendixes we sketch the derivation of the self-consistency equation for a mean-field confining potential allowing for the excluded volume effect in the system of chains, and find partition function of the quantum string used in Sec. II.

II. THERMODYNAMICS OF BOLALIPIDS

A. Microscopic model of flexible strings

Within a flexible string model, hydrophobic chains of lipid molecules are considered as flexible (effective) strings of finite thickness with a given bending rigidity. In a way there is no hydrophilic heads in the model. They participate indirectly via providing an extra part to the surface tension of the membrane that equilibrates lateral pressure contributed by the hydrophobic tails.

Let us introduce the deviation of the string from the z axis (see Fig. 2, vector $\mathbf{R}$) and consider oscillations of the string in the xz and yz planes as independent. The chain flexural rigidity is defined as [6] $K_f = EI$, where $E \approx 0.3$ GPa is the chain Young's modulus [7] and $I = A_0^2/4\pi$ is the (geometric) moment of inertia. The flexural rigidity can also be evaluated from the polymer theory [8] $K_f = k_B T l_p$, where $l_p \approx L/3$ is the chain persistence length [7] and k_B is the Boltzmann constant. Both estimates give approximately $K_f \approx k_B T L/3$ at chosen L and at $T = T_0$, where $T_0 = 300$ K is a reference temperature. We take $A_0 = 20$ Å^2 for the incompressible area per chain and $2L = 30$ Å for the bolalipid membrane thickness.
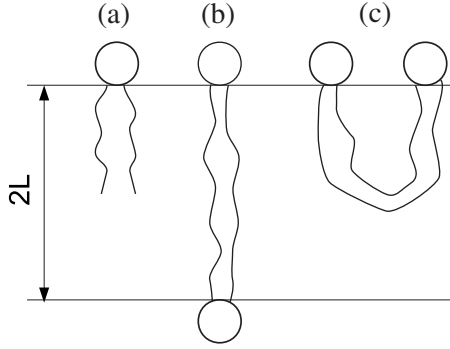
*sergeimoscow@online.ru

FIG. 1. (a) Monopolar lipid, e.g., phospholipid or glycolipid; (b) bipolar lipid, e.g., bolalipid; and (c) bolalipid in a so-called hairpin configuration, hairpin bolalipid. $2L$ is a thickness of hydrophobic region of the membrane. We take $2L = 30$ Å.

B. Energy functional

The energy functional of the chain is given by

$$E_t = \int_0^{2L} \left\{ \frac{\rho \dot{\mathbf{R}}^2(z)}{2} + \frac{K_f}{2} \left(\frac{\partial^2 \mathbf{R}(z)}{\partial z^2} \right)^2 + \frac{B}{2} \mathbf{R}^2(z) \right\} dz. \quad (1)$$

Here, the first term is a kinetic energy of the lateral (transverse) vibrations of the string, the second is a bending energy (see [6]), and the third one accounts for entropic interaction (effective repulsion induced by excluded volume) of neighboring chains. In a mean-field approximation we model it by a harmonic potential $U_{eff} = BR^2/2$, where B is a constant of interaction and we will find it later using a self-consistency equation (in Sec. II C). Vector $\mathbf{R}$ is a deviation of the center of string from the z axis (see Fig. 2). The choice of harmonic potential is justified since we assume finite "softness" of the effective "cage" created by the neighboring lipid chains in the limit of small chain deviations. A harmonic potential was considered in earlier work [9] for a semiflexible polymer confined along its axis. The elastic energy treatment of the molecular chains is especially well known in the theory of polymers (see, e.g., [10–12]). ρ in a first term of Eq. (1) is a linear density of mass: $\rho = m(\mathrm{CH}_2)N/2L$, where $m(\mathrm{CH}_2)$ is a mass of the hydrocarbon group and N is the number of hydrocarbon groups per chain (for numerical estimates we took $N = 18$; see [13]).

We assume that deviations of the string from the z axis are small in comparison with the string length, so that in Eq. (1) the gradient expansion of the chain's length to the lowest

TABLE I. According to the present model, the net effect of mere modification of conditions at the midplane region of bolalipid membrane with respect to monopolar lipid bilayer is as follows: it is more difficult to compress the bolalipid membrane area, and also its area expands less with temperature. Calculations are performed for membrane tension $\gamma = 30$ dyn/cm in the head group region.

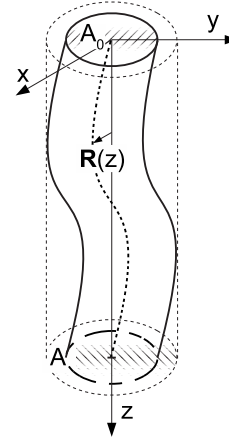| Parameter	Bolalipid	Monopolar lipid
K_a (erg/cm^2)	67.3	51.3
K_T (10^{-3} K^{-1})	1.4	1.8

FIG. 2. Hydrophobic chain as a flexible string of finite thickness. We consider deviations of the centers of the string, $\mathbf{R}(z)$. A_0 is an incompressible area of the chain and A is a mean area swept by the string. A mean-field confining potential allowing for the excluded volume effect of the surrounding chains is included in the model to keep area A per chain finite.

order is used. We will check the applicability of this assumption in the end of this section.

Boundary conditions for the string are as follows. The chain angle is fixed in the head group region [see Eq. (2)] and no total force is applied upon chain at the head group [see Eq. (3)]:

$$R'(0) = 0, \quad R'(2L) = 0, \quad (2)$$

$$R'''(0) = 0, \quad R'''(2L) = 0 \quad (3)$$

[these conditions, being symmetrical with respect to bolalipid heads (at $z = 0$ and at $z = 2L$), are in contrast with the boundary conditions used for a monolayer of thickness L that consists of monopolar lipids and forms one half of the bilayer lipid membrane of thickness $2L$ [5]: $R'(0) = 0$, $R'''(0) = 0$ and $R''(L) = 0$, $R'''(L) = 0$]. With these boundary conditions it is possible to rewrite potential energy of the string using self-adjoint operator [which is obtained by integration by parts of bending energy in Eq. (1)]:

$$\hat{H} = K_f \frac{\partial^4}{\partial z^4} + B. \quad (4)$$

Then the energy functional takes a form

$$E_t = \sum_{i=x,y} \frac{1}{2} \int_0^{2L} [\rho \dot{R}_i^2(z) + R_i(z) \hat{H} R_i(z) dz]. \quad (5)$$

Eigenfunctions of $\hat{H}$ are the normal modes of oscillation of the string, while its eigenvalues are the effective rigidities of those modes. We find eigenfunctions and eigenvalues by solving

$$\hat{H} R_n \equiv K_f \frac{\partial^4 R_n}{\partial z^4} + B R_n = E_n R_n. \quad (6)$$

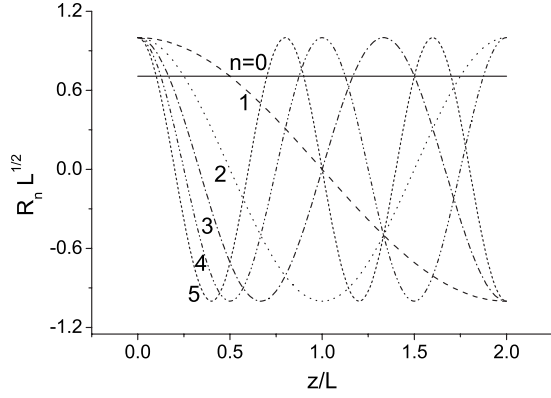With the boundary conditions (2) and (3) one obtains

FIG. 3. Several first ($n=0-5$) eigenfunctions $R_n(z)$ of $\hat{H}$ [see Eq. (8)]. Eigenfunctions are the normal modes of oscillation of the bolalipid chain. $z=0$ and $z=2L$ are the membrane interfaces (more precisely, they are the boundaries between heads and tails), $z=L$ is the membrane midplane, and $L=15$ Å is monolayer thickness.

$$E_n = B + \frac{k_n^4 K_f}{L^4}, \quad k_n = \pi n/2, \quad n \geq 1, \quad E_0 = B, \qquad (7)$$

$$R_N(z) = c_n \cos(k_n z/L), \quad n \geq 1, \quad R_0(z) = \sqrt{\frac{1}{2L}}, \qquad (8)$$

where $c_n = \sqrt{1/L}$ and $\lambda_n = 2\pi L/k_n$ is the wavelength. Several eigenfunctions are shown in Fig. 3. Then, an arbitrary time-dependent conformation of the string $R_x(z,t)$, which describes deviation from the straight line (aligned along the z axis), as well the energy E_t of this conformation, can be expanded over the eigenfunctions $R_n(z)$ and eigenvalues E_n, respectively,

$$R_x(z,t) = \sum_{n \geq 0} C_n(t) R_n(z),$$

$$\dot{R}_x = \sum_{n \geq 0} \dot{C}_n R_n, \quad E_t = \frac{1}{2} \sum_{n \geq 0} \{\rho \dot{C}_n^2 + C_n^2 E_n\}, \qquad (9)$$

where $C_n(t)$ are the time-dependent amplitudes of the expansion.

C. Self-consistency

Using standard statistical formula for the mean, we express $\partial F/\partial B$ via mean area swept by a chain in the xy plane, where $F = -k_B T \ln(Z)$ is a free energy of the string without surface energy. We describe this stepwise below. Namely, the partition function Z of the string is a path integral over all chain conformations:

$$Z = \int \exp\left(-\frac{E[\dot{\mathbf{R}}(z), \mathbf{R}(z)]}{k_B T}\right) D\dot{R}_x DR_x D\dot{R}_y DR_y$$

$$= \left[\int \exp\left(-\frac{E[\dot{R}_x(z), R_x(z)]}{k_B T}\right) D\dot{R}_x DR_x\right]^2$$

$$= Z_x^2. \qquad (10)$$

The second equality in Eq. (10) holds when we consider x and y deviations as independent, which is true for laterally isotropic membrane. Calculating $\partial F/\partial B$ one obtains

$$\frac{\partial F}{\partial B} = k_B T \frac{\int \left\{\int_0^{2L} R_x^2(z) \exp\left[\frac{-E(R_x(z))}{k_B T}\right] dz\right\} DR_x}{\int \exp\left[\frac{-E(R_x(z))}{k_B T}\right] DR_x}$$

$$= 2L\langle R^2 \rangle, \qquad (11)$$

where $\langle R^2 \rangle = (\sqrt{A} - \sqrt{A_0})^2/\pi$ (see Appendix A for a derivation), A is a mean area swept by the fluctuating string, and A_0 is an incompressible area of the string (see Fig. 2).

On the other hand, we calculate the partition function Z of the string explicitly as a path integral over all chain conformations. In order to perform this calculation we express an arbitrary chain conformation as an expansion series over the eigenmodes $R_n(z)$ and then reduce the path integral to an integral on the space of the expansion amplitudes $C_n(t)$ defined in Eq. (9). In the limit of classical mechanics of the string, an account of kinetic energy of the string is taken by an independent integral over the conjugated momenta $p_n = \rho \dot{C}_n$:

$$Z_x = \int_{-\infty}^{\infty} \prod_{n \geq 0} \exp\left(-\frac{p_n^2}{2\rho k_B T} - \frac{C_n^2 E_n}{2 k_B T}\right) \frac{dp_n dC_n}{2\pi\hbar}$$

$$= \prod_{n \geq 0} \frac{k_B T}{\hbar} \sqrt{\frac{\rho}{E_n}}$$

$$= \prod_{n \geq 0} \frac{k_B T}{\hbar \omega_n}, \qquad (12)$$

where $\omega_n \equiv \sqrt{E_n/\rho}$. It is important that the latter expression for ω_n in the limit of a free string, $B \equiv 0$, gives the well-known bending wave spectrum of the Euler's beam [6]: $\omega_n = \sqrt{EI\tilde{k}_n^4/\rho}$ (with $\tilde{k}_n \equiv k_n/L$), as it follows from Eq. (7) and expression for the bending rigidity $K_f = EI$ mentioned above. Hence, by including kinetic energy of the chain into the energy functional E_t, we obtain correct dimensionless expression for partition sum in Eq. (12). The unit of "volume per state" in momentum space, $2\pi\hbar$, which normalizes integration over dp_n, is arbitrary in classical mechanics; but we fix its value using correspondence with the quantum statistical physics (see Appendix C).

Using Eqs. (10)–(12) and $F = -k_B T \ln(Z)$ we find the following expression for the free energy of the string that models mechanical motion of a bolalipid chain (not including surface energy):

$$F_t = -2k_B T \sum_{n=0}^{n_{max}} \ln\left(\frac{k_B T}{\hbar \omega_n}\right), \qquad (13)$$

where we take into account that summation over the eigenmodes n has an "ultraviolet cutoff" n_{max}, i.e., the shortest possible wavelength is limited from below due to a finite number of CH_2 groups. As mentioned above, we take 18 CH_2 groups for "half layer" of bolalipid membrane (i.e., 36

groups for the single bolalipid chain). According to this, the cutoff number would be $n_{max} = N(CH_2) - 1$. Yet, the effective n_{max} is even smaller: compactifying 36 CH_2 groups in a $2L = 30$ Å-thick membrane means that a chain has some sort of helical structure. The reason is that, because the length of the CH_2-CH_2 bond is 0.1265 nm [14], the length of a straight chain would be 45 Å instead of 30 Å. This means that we work with some effective strings that possess the same linear density ρ as the real hydrocarbon chains in the membrane, but the number of effective segments is less than the number of CH_2 groups. It is not quite clear how many segments might be ascribed to effective string. Assuming a segment having three CH_2 groups we obtained number of segments in the bolalipid chain equal to 12 and, hence, $n_{max} = 12 - 1 = 11$ (where 1 takes into account zero mode). It is worth mentioning that with such n_{max} we stay within the classical mechanics at room temperatures: $\hbar \omega_{n_{max}} / (k_B T) = 0.29 \ll 1$.

Differentiating expression in Eq. (13) with respect to B and equating the result with Eq. (11), we obtain the self-consistent dependence of the interaction constant B [see Eq. (1)] on the mean area per chain A in the xy plane (see Appendix B for the derivation):

$$B = \frac{K_f}{4L^4 \nu^{4/3} (\sqrt{a} - 1)^{8/3}} \sim \frac{T^{4/3}}{K_f^{1/3} (\sqrt{a} - 1)^{8/3}}, \quad (14)$$

where the dimensionless parameter $\nu = K_f A_0 / \pi k_B T L^3$ is introduced and Flory's relation is assumed: $K_f \approx k_B T L / 3$. Hence, enhancement of bending rigidity K_f, at some fixed temperature T and area a, suppresses the entropic repulsion coefficient B, as one would, indeed, expect.

D. Equation of state

The total free energy per bolalipid chain in the membrane is the sum of the free energy of hydrophobic part (hydrocarbon chain between the opposite monopolar heads of bolalipid) and a surface energy: $F_\Sigma = F_t(A) + 2\gamma A$. Here, γ represents the contribution to the surface tension from the polar heads region, and the factor 2 accounts for two surfaces of the membrane of bolalipid molecules. In the equilibrium,

$$\left(\frac{\partial F_\Sigma}{\partial A} \right)_T = 0 \Rightarrow \left(\frac{\partial F_t}{\partial A} \right)_T + 2\gamma = 0. \quad (15)$$

This means zero total surface tension of the self-assembled membrane. For brevity, everywhere below we call polar head contribution γ just a surface tension.

Notice that

$$P_t = -\left(\frac{\partial F_t}{\partial A} \right)_T, \quad (16)$$

where P_t is a total pressure produced by hydrophobic chains, i.e., equilibrium condition simply states that repulsion between chains should be balanced by the surface tension contributed by the polar heads. From Eqs. (13) and (14) we obtain
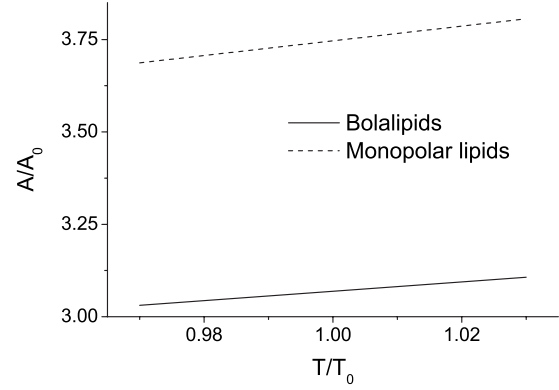

FIG. 4. Calculated equilibrium area per chain as a function of temperature for a monolayer of bolalipids (solid line) and a bilayer of monopolar lipids (dashed line). γ is a surface tension, $A_0 = 20$ Å^2 is incompressible chain cross-section area, and $T_0 = 300$ K. Slope of the bolalipid membrane curve is a bit less than that one of the monopolar lipid membrane.

$$P_t^{bola} = \frac{2k_B T}{3A_0 \nu^{1/3} \sqrt{a} (\sqrt{a} - 1)^{5/3}}. \quad (17)$$

Once the $B(A)$ dependence and equilibrium area per chain are found, one can calculate free energy per chain [see Eq. (13)]. This allows us to derive further thermodynamic quantities of interest.

One can calculate the isothermal area compressibility modulus,

$$K_a = -A \left(\frac{\partial P_t}{\partial A} \right)_T, \quad (18)$$

and the coefficient of thermal area expansion,

$$K_T = \frac{1}{A} \left(\frac{\partial A}{\partial T} \right)_P. \quad (19)$$

Also, using Eq. (17) and condition (15) one can find equilibrium area per hydrophobic chain of bolalipid membrane with the given surface tension γ at a given temperature, plotted in Fig. 4. We choose $\gamma = 30$ erg/cm^2 [15,16].

As it follows from the plot (see Fig. 4), in the lateral direction the chains in a bolalipid membrane tend to pack noticeably more compact in comparison with the chains in a monopolar lipid bilayer of the same thickness at the same temperature. Another calculated result is presented in Fig. 5. The pressure-area isotherm $P_t(A)$ for bolalipid membrane given by Eq. (17) is illustrated and compared with the pressure-area isotherm calculated for monopolar lipid bilayer (compare [5]). It is obvious from the plot that bolalipid membrane has smaller lateral (hydrophobic region) pressure than the monopolar lipid bilayer at the same area per chain and thickness. We investigate the underlying reasons of these (inter-related) differences in the following section.

E. Thermodynamic properties

In order to acquire deeper understanding of the thermodynamic properties that bolalipid membrane possesses on me-
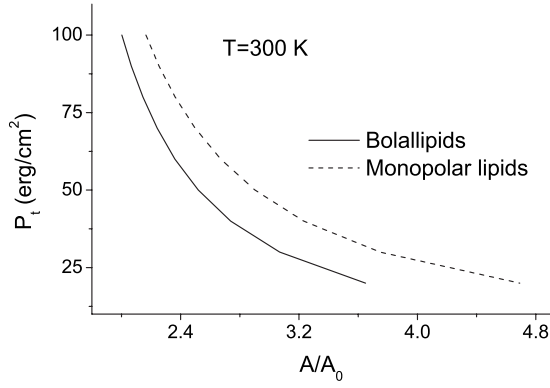
FIG. 5. Total lateral pressure produced by hydrophobic tails of bolalipid (solid line) and monopolar lipid (dashed line) membranes as a function of area per chain; A_0 is the same as in Fig. 4.

soscopic scale, we calculated chain orientational order parameter $S(z)$ as a function of the depth (z coordinate) inside the lipid membrane defined as

$$S(z) = \tfrac{1}{2}[3\langle\cos^2\theta(z)\rangle - 1], \qquad (20)$$

where $\theta(z)$ gives the distribution of the tangent angle of the chain across the bolalipid membrane. Straight (ordered) chain possesses $\theta \equiv 0$ and $S(z) \equiv 1$. In the limit of small deviations from the straight line, $\theta \ll 1$, considered in our model, the order parameter can be expressed using the following relations:

$$\langle\cos^2\theta(z)\rangle \approx 1 - \langle\tan^2\theta(z)\rangle, \qquad (21)$$

$$\langle\tan^2\theta(z)\rangle = 2\langle[R'(z)]^2\rangle = 2k_BT\sum_{n=0}\frac{[R'_n(z)]^2}{E_n}, \qquad$$

so that finally we obtain

$$S(z) \approx 1 - 3k_BT\sum_{n=0}\frac{[R'_n(z)]^2}{E_n}, \qquad (22)$$

where the factor 2 in front of $\langle[R'(z)]^2\rangle$ in Eq. (21) arises after independent summation of the deviations in the perpendicular planes $\{x,z\}$ and $\{y,z\}$ (see Fig. 2). The result is plotted in Fig. 6(a).

The orientational order of bolalipid in the depth of the membrane is significantly higher than that of the monopolar lipid. Especially pronounced difference is achieved in the midplane region (or monolayer's interface for the bilayer built from monopolar lipids). While the midplane-centered segments of the bolalipid molecule are correlated with their neighbors due to intersegment links, the monopolar lipid chains posses free ends at the monolayers interface, and therefore contribute more to the entropy of the hydrophobic part of the bilayer. It is possible to check that this is indeed the case by calculating the lateral pressure profile, i.e., the distribution of pressure across the bolalipid membrane. By substituting the expression for the free energy (13) into Eq. (16) one finds
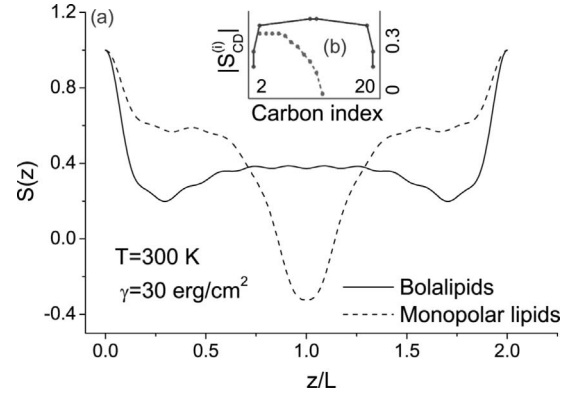

FIG. 6. (a) Calculated orientational order parameter of the flexible strings modeling bolalipid membrane (solid line) and monopolar lipid membrane (dashed line); normalization length L, used as z-coordinate scale, is the same as in Fig. 3. Result for the monopolar lipid membrane is obtained in [5] (see details in Sec. III A); (b) experimental NMR data by [18] of segmental order parameter for hydrophobic part of a membrane; the upper curve is for bolalipid membrane, while the lower curve is for one monolayer of lipid bilayer membrane built from monopolar lipids.

$$P_t = -k_BT\sum_{n=0}\left(\frac{\partial E_n}{\partial A}\right)_T\frac{1}{E_n}. \qquad (23)$$

We may consider P_t as an integral of the lateral pressure distribution (profile) function, $\Pi_t(z)$, over the hydrophobic thickness of the lipid membrane (i.e., over bilayer in the case of monopolar lipids and monolayer in the case of bolalipids):

$$P_t \equiv \int \Pi_t(z)dz. \qquad (24)$$

In order to find out $\Pi_t(z)$ defined this way, it is possible to use the following formal trick. Namely, the dependence on area A of E_n arises via dependence of the "potential" $B(A)$ that enters operator $\hat{H}$ in Eq. (6). One may in addition formally consider $B(A)$ as being a z-dependent function. Then, a well-known relation from the Hamiltonian operator perturbation theory [19], used in the second equality below, leads to the following equation:

$$\left(\frac{\partial E_n}{\partial A}\right)_T \equiv \int\left(\frac{\delta E_n}{\delta B}\right)_T\left(\frac{\partial B}{\partial A}\right)_T\frac{dz}{1} = \int R_n^2(z)\left(\frac{\partial B}{\partial A}\right)_T dz, \qquad (25)$$

where 1 means unit length. Now, substituting Eq. (25) into Eq. (23) we find an analytical expression for the lateral pressure profile from the relation

$$P_t = -\int k_BT\sum_{n=0}\frac{R_n^2(z)}{E_n}\left(\frac{\partial B}{\partial A}\right)_T dz \equiv \int \Pi_t(z)dz. \qquad (26)$$
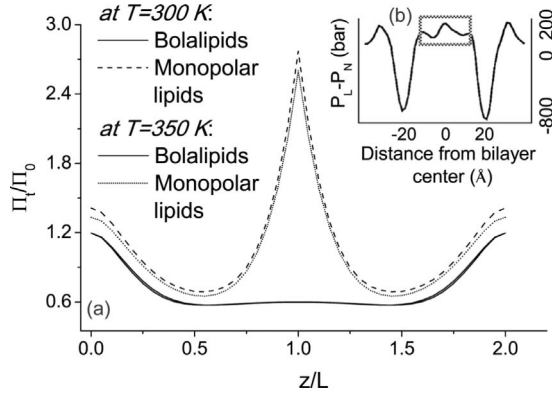
Hence, finally,

FIG. 7. (a) Lateral pressure profile of the chains of bolalipid (solid line) and monopolar lipid (dashed and dotted lines) membranes at $T=300$ and 350 K respectively, with unchanged γ. Bolalipid chain profile is practically the same at both temperatures. Normalization length L, used as z-coordinate scale, is the same as in Fig. 3, $\Pi_0=\gamma/L=2\times10^8$ dyn/cm². (b) Numerical results of atomistic simulations for lateral pressure profile of the monopolar lipids by [17]; the rectangle allocates thickness interval relevant to our model calculations. See Sec. III A, for validity of calculated central peak and other details.

$$\Pi_t(z) = -k_B T \left(\frac{\partial B(A)}{\partial A}\right)_T \sum_{n=0}^{} \frac{R_n^2(z)}{E_n}. \qquad (27)$$

Comparison of Fig. 7(a) with Fig. 6(a) shows that entropic repulsion rules the lateral pressure profile. In particular, in the bolalipid case (solid line), the absence of the lateral pressure peak is directly related to the absence of the orientational disorder in that region, which is manifest in Fig. 6(a) [absence of the order parameter dip (solid line)]. At the same time, the midplane peak in Fig. 7(a) (dashed and dotted lines) at $z/L=1$ corresponds to the midplane dip in the orientational order parameter curve (dashed line) of the monopolar lipids bilayer in Fig. 6(a). Local peaks of pressure at the membrane surfaces ($z=0$ and $z=2L$) in the lateral pressure profiles in Fig. 7(a) are due to collisions of hydrophobic heads with each other and look similar for bolalipid and monopolar lipid membranes. We believe that pressure peak in the midlayer region occurs due to free ends of monopolar lipid chains, which are absent in the bolalipid membrane where pressure peak is vanishing. Comparison of the lateral pressure profiles at $T=300$ K and $T=350$ K calculated under fixed parameter γ indicates that in our model bolalipids are less sensitive to increase in temperature than the monopolar lipids. This result is preliminary since it does not take, so far, into account the possibility of new conformations that may become accessible for the lipids at higher temperatures (including protrusion of molecules into water, stretched-to-hairpin molecule transitions, etc.), as well as possible changes in parameter γ with temperature.

F. Verification of the small deviation approximation

It is known that in a classical limit the mean value of the energy corresponding to the one oscillating degree of free-dom is $k_B T$. Projecting this wisdom onto our model, we conclude that

$$E_n \langle C_n^2 \rangle = k_B T. \qquad (28)$$

Taking into account that we consider oscillations of the chain in the x and y directions as independent, we can calculate the average of the chain's fluctuation:

$$\langle \mathbf{R}^2(z) \rangle = \langle R_x^2(z) \rangle + \langle R_y^2(z) \rangle$$
$$= 2\sum_n \langle C_n^2 \rangle R_n^2(z) = 2k_B T \sum_n \frac{R_n^2(z)}{E_n}, \qquad (29)$$

where in the last equality we used Eq. (28). To proceed with this we estimate $R_n^2 \sim 1/L$ [see Eq. (8)] and $\Sigma_n 1/E_n \gtrsim 1/B$ since all $E_n > 0$ and $E_0 = B$. One can notice that a variation of the potential energy of the chain (not including surface energy) associated with the variation of area δA is of the order of $2BL\delta A$, while on the other hand, it is equal to the work against the pressure: $P\delta A$. Here, $P=2\gamma$ and γ is the tension at polar heads. So, we estimate $B \sim \gamma/L$ and substitute this into Eq. (29) that then leads to

$$\frac{\sqrt{\langle \mathbf{R}^2(z) \rangle}}{2L} = \sqrt{\frac{k_B T}{4\gamma L^2}} = 0.12. \qquad (30)$$

This latter estimate proves that with our choice of parameters we are working in a limit of small lateral deviations with respect to the layer thickness. On the other hand, as is shown in the next section, this approximation fails in the vicinity of monolayer interface, so that our results in this particular (narrow) region should be considered as merely qualitative.

III. DISCUSSION

In this section we discuss in more detail the applicability of our approximation of small lateral deviations in the vicinity of midplane region ($z/L=1$) of the bilayer membrane. We also compare results obtained in Sec. II with the results for the monopolar lipid membrane obtained earlier [5], as well as with the results of other studies [4,17]. After that, we explain approximate method that was used to calculate lateral pressure profile in the asymmetric bolalipid membrane with differing concentrations of hairpin bolalipids in the monolayers. Finally, we discuss relationship between free energy of the membrane and flexural rigidity of lipid chain in our model.

A. Lipid chain deviations and order parameter in the midplane region

Comparison of our analytical results with numerical results of atomistic simulations, both presented in Fig. 7, raises a question about the applicability of the approximation of small chain deviations in the midplane region. An estimate for monopolar lipids, obtained similarly to the estimate expressed in Eq. (30) for bolalipids, is as follows (with a tension at polar heads region being $\gamma=30$ dyn/cm):
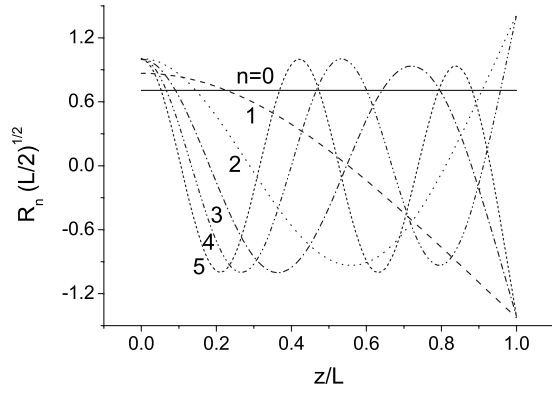
FIG. 8. Eigenfunctions $R_n(z)$, $n = 0-5$, of the potential-energy operator (4) of the monopolar lipids. Comparison with characteristic value R_0 (solid line is at $R_0 \sqrt{L/2} = 1/\sqrt{2}$) indicates that the estimate $R_n^2 \lesssim 2/L$, which was used in Eq. (31), does not work in the midplane region (at $z = L$). Normalization length L, used as z-coordinate scale, is the same as in Fig. 3.

$$\frac{\sqrt{\langle \mathbf{R}^2(z) \rangle}}{L} = \sqrt{\frac{2k_B T}{\gamma L^2}} = 0.35. \qquad (31)$$

At first glance, the estimate should indicate that the condition of smallness of the deviations is fulfilled for any z/L. But, this result was obtained using an estimate $R_n^2 \lesssim 2/L$, which works well except in the narrow region around midplane, $z/L = 1$. In the latter region the eigenfunctions increase appreciably (see Fig. 8) beyond $2/L$, and small deviation approximation is not justified. This suggests that the midplane pressure peak in Fig. 7(a) for monopolar lipids in reality might be not that high. For comparison of our analytical results with molecular dynamics calculation, we present a plot from [17] in Fig. 7(b), which is in good qualitative correspondence with our results in Fig. 7(a) (dashed and dotted lines), except for the midplane region, where they indeed obtained just a flat hill-like plateau, instead of the peak in Fig. 7(a) by the reasons explained above. By the same reason of big lateral deviations of monopolar lipid chains at the midplane, our results for the value of the order parameter of the monopolar lipids at the dip (see Fig. 6) are only qualitatively correct since, e.g., at $S(z) = 0.5$ corresponding to $\theta = 0.8$, the relative error of substitution of θ^2 with $\tan^2 \theta$, used in Eq. (21), is ~20%.

Calculated profiles of the order parameter as a function of the z coordinate (along the membrane thickness) for bolalipid and monopolar lipid membranes presented in Fig. 6(a) are in good qualitative agreement with the NMR experiments [18]; see the inset in Fig. 6(b). In this inset the order parameters of bolalipid chains (upper curve) and monopolar lipid chain (lower curve) are plotted as functions of the consecutive numbers of the hydrocarbon groups (segments) constituting the chains. The seeming discrepancy of the calculated $S(z)$ behavior at the ends of the z/L interval in A and at the ends of carbon-numbered interval in B is due to a different choice of the origin. Namely, in our model the head groups are located at $z = 0, 2L$, while experimental NMR data are obtained only in the region *between* the head groups. We
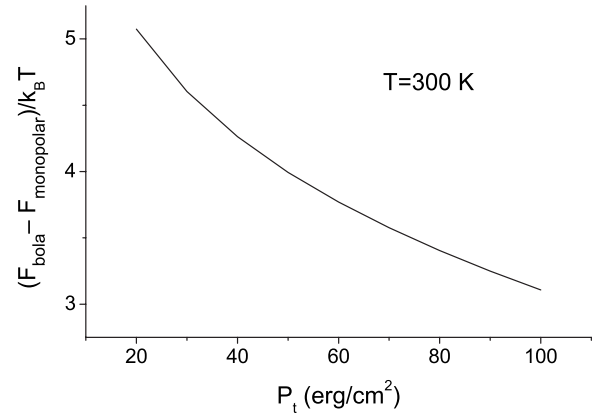

FIG. 9. Our model implies that if a bolalipid differs from a monopolar lipid only by the linked tails condition (see Sec. I, Fig. 1), then it has greater free energy F.

should mention here that unlike in Fig. 6(a), experimental curve in Fig. 6(b) for bolalipid molecule is going above the curve for monopolar lipid inside the whole interval of carbon numbers. We speculate that this might be due to different flexural moduli of the bolalipids and monopolar lipids studied in [18], while for our calculation the "monopolar" lipids are obtained from "bipolar" by merely cutting the (model) string into two halves with simultaneous changes in the boundary conditions at the cut ends [as explained after Eq. (3)].

B. Comparison of thermodynamic coefficients

We had calculated the chain contribution to isothermal area compressibility modulus using Eq. (18) and coefficient of thermal area expansion for bolalipid membrane (see Table I). Calculated coefficients of area expansion lie within the range of measured values ($\approx 2 \times 10^{-3}$ K^{-1} [16]), while calculated chain-induced area compressibility moduli are lower than experimental values (≈ 240 erg/cm^2 [16]). This suggests that the head group region is more rigid than the hydrophobic core.

C. Comparison with other study

Our model suggests that under equal conditions, except at the monolayer interface (i.e., at the middle of the membrane thickness), the free energy per bolalipid is greater than that one per two monopolar lipids (see Fig. 9). Under the "conditions" we understand the number of CH$_2$ groups, bending rigidity K_f of the chain, and incompressible area per chain, A_0.

In [4] the authors obtained an opposite result for the free energy: the free energy per bola is less than the one per two monopolar lipids. We found that we can achieve quantitative agreement with [4] by assuming that the monopolar lipid chain rigidity is twice the bolalipid's one. Other way to achieve agreement is to increase an incompressible area of monopolar lipid chain with respect to the bolalipid one.

Hypothetically the difference of the bola and monopolar lipid chain rigidities could be caused by the following rea-
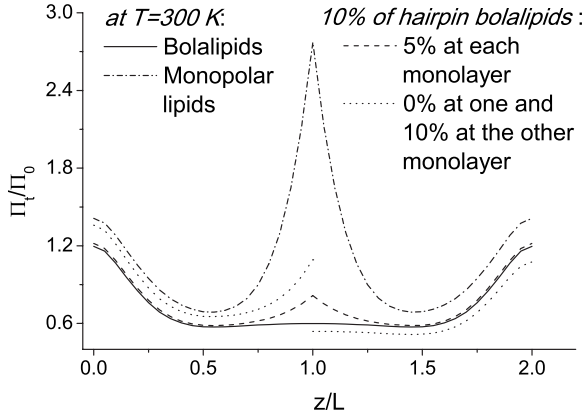
FIG. 10. A hairpin bolalipid is substituted by two extra monopolar lipids within a monolayer. Hence, contribution to the lateral pressure from the hairpin bolalipids is substituted by the contributions of an appropriate number of extra monopolar lipids.

son: in case the monopolar lipids have greater number of CH_2 groups per unit length than the bolalipids, this may enhance the "helical" structure of the monopolar lipid chain, so that effective string, which models monopolar lipid, should have greater bending rigidity and/or greater incompressible area than effective string that models bolalipid.

D. Asymmetric bolalipid membranes

Bolalipid could have both heads on one interface. Then it is called hairpin bolalipid [see Fig. 1(c)]. When concentrations of hairpin bolalipids in the monolayers are different we call the membrane asymmetric.

To mimic asymmetry of bolalipid membrane with small admixture of hairpin bolalipids, we substitute a hairpin bolalipid by two monopolar lipids placed in the same monolayer. Figure 10 (dashed and dotted lines) represents lateral pressure profiles of several asymmetric membranes calculated using this substitution. The pressure profiles are sums of partial lateral pressure contributions of "mimicking monopolar lipids" and bolalipids (in transmembrane state). Certainly, the segments of the hairpin bolalipid chain in the membrane are not moving independently and, therefore, their freedom to meander is restricted in comparison with the segments of the tails of two independent neighboring monopolar lipids. Nevertheless, we believe that this calculation may provide a useful hint for the lateral pressure profile in a bolalipid membrane with small admixture of hairpin bolalipid molecules.

E. Energy dependence on rigidity: Absolutely rigid strings

Within our model we found that the total free energy of the string increases with its rigidity. This effect is not that obvious from the start. But, using Eqs. (7) and (13) and the definition of ω_n after Eq. (12), we have $F \propto \ln(\sqrt{K_f})$, and hence free energy increases with K_f.

In order to clarify this effect we considered a limiting case—strings with infinite rigidity, i.e., rods. We derived thermodynamical properties of the "membrane of rods" and
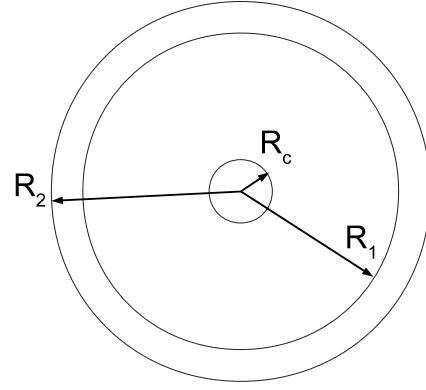

FIG. 11. Mean area, swept by the chain. See Appendix A for notation.

the conclusion remains the same: the greater is the rigidity, the greater is free energy per chain.

APPENDIX A: MEAN AREA

In order to find $\langle R^2 \rangle$, where angular brackets denote the mean, consider a mean area swept by the centers of the chains (as a function of the z coordinate; see Fig. 2). It is equal to $\pi \langle R^2 \rangle$. Let us introduce $R_c = \sqrt{\langle R^2 \rangle}$. At the same time chain, as a whole, sweeps the area $A = \pi R_2^2$. Let us also introduce $\pi R_1^2 = A_0$. R_c, R_1, and R_2 are related by the condition $R_c = R_2 - R_1$ (see Fig. 11). This allows us to find

$$\langle R^2 \rangle = (\sqrt{A} - \sqrt{A_0})^2/\pi. \qquad (A1)$$

APPENDIX B: $B(A)$ dependence

Calculation of $(\partial F/\partial B)_T$ using Eq. (13) gives

$$\left(\frac{\partial F}{\partial B}\right)_T = k_B T \sum_{n=0}^{\infty} \frac{1}{B + k_n^4 K_f/L^4} = \frac{2L(\sqrt{A} - \sqrt{A_0})^2}{\pi}, \quad (B1)$$

where $k_n = \pi n/2$ and the last equality is valid due to Eqs. (11) and (A1). It is convenient to introduce dimensionless parameters

$$a = A/A_0, \quad b = \frac{L^4}{K_f}B, \quad \nu = \frac{K_f A_0}{\pi k_B T L^3}, \qquad (B2)$$

where $L \sim 15$ Å is the chain length, $A_0 \sim 20$ Å^2 is the "incompressible area" of the chain cross section, and the chain flexural rigidity $K_f \cong k_B T L/3$ at $T \approx T_0 = 300$ K. Using these estimates we obtain for the dimensionless parameter $\nu \cong 0.009$.

With this notation the self-consistent equation (B1) takes the form

$$\sum_{n=0} \frac{1}{b + k_n^4} = 2\nu(\sqrt{a} - 1)^2. \tag{B3}$$

The terms in the sum on the left-hand side of Eq. (B3) decrease fast with growing n, and we can use integration instead of summation over n. For example, for the effective tension $P_{eff} = 30$ dyn/cm, we have $b \approx 250$, while $k_1^4 \approx 6$. In this regime we can solve Eq. (B3) analytically by substituting summation over n with integration, which yields

$$\sum_{n=0} \frac{1}{b + k_n^4} \approx \frac{1}{2} \int_{-\infty}^{\infty} \frac{dn}{b + k_n^4} = \frac{1}{\sqrt{2}b^{3/4}}, \tag{B4}$$

where we took integral using residue theory. This leads to

$$\frac{1}{\sqrt{2}b^{3/4}} = 2\nu(\sqrt{a} - 1)^2, \tag{B5}$$

and, finally,

$$b = \frac{1}{4\nu^{4/3}(\sqrt{a} - 1)^{8/3}}. \tag{B6}$$

Returning to dimensionalized parameters one finds Eq. (14).

In the case with monopolar lipids the equation is as follows:

$$\frac{1}{b} + \frac{1}{2\sqrt{2}b^{3/4}} = \nu(\sqrt{a} - 1)^2. \tag{B7}$$

But in contrast to Eq. (B3) it has more complicated dependence on b. In the previous paper [5] only high value was considered for the surface tension $\gamma = 100$ dyn/cm, which leads to $b \sim 10^3$. Hence, it was possible to neglect the first term in Eq. (B7). Since now b proves to be not that big, we treated this equation numerically.

APPENDIX C: QUANTUM LIMIT

Here we obtain Eq. (13) as a limit of a quantum formula. In quantum mechanics harmonic oscillations have quantized energies: $E_p = \hbar\omega(p + 1/2)$. Hence, the partition function of quantized oscillations of a string in the xz plane is given by

$$Z_x = \prod_{n=0} Z_{xn}$$

$$= \prod_{n=0} \sum_{p=0} \exp\left(-\frac{h\omega_n(p + 1/2)}{k_B T} \right)$$

$$= \prod_{n=0} \left[\frac{\exp\left(-\frac{\hbar\omega_n}{2k_B T} \right)}{1 - \exp\left(-\frac{\hbar\omega_n}{k_B T} \right)} \right], \tag{C1}$$

and the free energy is equal to

$$F = -2k_B T \ln(Z_x) = \sum_{n=0} \hbar\omega_n + 2k_b T \sum_{n=0} \ln\left[1 - \exp\left(-\frac{\hbar\omega_n}{k_B T} \right) \right], \tag{C2}$$

which gives formula (13) in the classical limit $\hbar\omega_n/k_B T \ll 1$.

[1] C. Woese, O. Kandler, and M. Wheelis, Proc. Natl. Acad. Sci. U.S.A. **87**, 4576 (1990).

[2] David H. Thompson *et al.*, J. Am. Chem. Soc. **114**, 9035 (1992).

[3] P. Raven *et al.*, *Biology*, 8th ed. (McGraw-Hill, Dubuque, IA, 2008).

[4] Gabriel S. Longo, David H. Thompson, and I. Szleifer, Biophys. J. **93**, 2609 (2007).

[5] S. I. Mukhin and S. Baoukina, Phys. Rev. E **71**, 061918 (2005).

[6] L. D. Landau and E. M. Lifshitz, *Theory of Elasticity* (Pergamon, Oxford, 1970).

[7] Young's modulus is by definition $E = P_z/u_{zz}$, where P_z is a pressure along the z axis and u_{zz} is a strain tensor component along the z axis. Hence, the modulus could be estimated by calculating deformation corresponding to conformational change of one link from trans to gauche conformation. Energy of such transformation is $\Delta E \approx k_B T$. The strain is $u_{zz} = \Delta L/2L$. Then pressure could be written as $P_z = \Delta E/\Delta L A_0$, where A_0 is a chain's incompressible area. Obviously, ΔL is comparable to the size of a CH_2 group of a bolalipid chain. Hence, roughly, we estimate $\Delta L = 2L/N$, where N is number of groups in the chain of a length $2L$. When all put together, the above estimates lead to $E \approx 0.3$ GPa and the bending rigidity is then $K_f = EI = 1 \times 10^{-30}$ J m. Flory's formula gives roughly the same result: $K_f = k_B T L/3 \approx 2 \times 10^{-30}$ J m.

[8] D. Nelson, *Defects and Geometry in Condensed Matter Physics* (Cambridge University Press, Cambridge, UK, 2002).

[9] T. W. Burkhardt, J. Phys. A **28**, L629 (1995).

[10] P. J. Flory, J. Chem. Phys. **17**, 303 (1949).

[11] P. G. de Gennes, *Scaling Concepts in Polymer Physics* (Cornell University Press, Ithaca, NY, 1979).

[12] H. Kleinert, *Path Integrals in Quantum Mechanics, Statistics and Polymer Physics*, 2nd ed. (World Scientific, Singapore, 1995).

[13] A. B. Rubin, *Biophysics of Cellular Processes*, Biophysics Vol. 2 (The University Publishing House, Moscow, 2000) [in Russian].

[14] J. N. Israelachvili, *Intermolecular and Surface Forces*, 2nd ed. (Academic, New York, 1992).

[15] D. Marsh, Biochim. Biophys. Acta **1286**, 183 (1996).

[16] E. Lindahl and O. Edholm, J. Chem. Phys. **113**, 3882 (2000).

[17] J. Gullingsrud and K. Schulten, Biophys. J. **86**, 3496 (2004).

[18] D. P. Holland *et al.*, J. Am. Chem. Soc. **130**, 4584 (2008).

[19] L. D. Landau and E. M. Lifshitz, *Quantum Mechanics* (Pergamon, Oxford, 1970).